Journal of Zhejiang University-SCIENCE A (Applied Physics & Engineering) *2022 23(8):621-638*
www.jzus.zju.edu.cn; www.springer.com/journal/11582
E-mail: jzus_a@zju.edu.cn

Research Article

https://doi.org/10.1631/jzus.A2100435

How fast is it to city centers? The average travel speed as an indicator of road traffic accessibility potential

Xiao-guang RUAN✉

College of Geomatics and Municipal Engineering, Zhejiang University of Water Resources and Electric Power, Hangzhou 310018, China

Abstract: Transportation is the lifeblood of a modern metropolis. Accessibility generally refers to the interconnection between nodes in a regional traffic network. The purpose of the paper is to obtain more realistic and accurate measures of travel speed and to study the road traffic accessibility potential in cities. This study proposes a method for analyzing road traffic accessibility potential which is based on the average travel speed to city centers in off-peak times and which ranks 80 cities around the world. Based on the Suomi National Polar-Orbiting Partnership satellite's visible-infrared imaging radiometer suite (NPP-VIIRS) night-time light data, urban built-up areas and city centers were extracted. Further, with the aid of the Google Maps application programming interface (API) network crawling technique, travel times and travel distances for several optimal routes to city centers by car were obtained. Feasible proposals for improving road traffic accessibility and planning urban transportation in different cities are presented. The proposed method offers a new possibility of analyzing traffic accessibility using internet data and geo-spatial methods.

Key words: Traffic accessibility; Google Maps application programming interface (API); Travel speed; Road traffic network; Geographic information system (GIS)

1 Introduction

The concept of accessibility, first proposed by Hansen (1959), is the ability to interact between nodes in transportation networks. Accessibility is generally used to describe the interactions between land-use and transport systems (Geurs and van Wee, 2004). Accessibility can be simply explained as the convenience of using a particular transportation system to reach a designated location from a certain location (Silva and Pinho, 2010). It is a common indicator for evaluating transportation networks and traffic locations (Kwan et al., 2003). Road infrastructure is the lifeblood of urban economic development (Démurger, 2001). The improvement of road traffic accessibility is an important factor in promoting economic activities (Odoki et al., 2001). Research on accessibility mainly focuses on spatial distribution, the characteristics of spatio-temporal evolution, the impact on regional economic development, etc. (Spence and Linneker, 1994; Gutiérrez et al., 1996). These studies cover ground transportation (roads and railways), maritime routes, and air routes, ranging from cities to regions to countries (Sathisan and Srinivasan, 1998; Bowen, 2000). The characteristics can be summarized as multi-scale, multi-model, and multi-indicator (Sathisan and Srinivasan, 1998; Bowen, 2000; Chen J et al., 2017).

In previous studies, there are many methods and indicators to evaluate accessibility, including: (1) network density, (2) spatial barriers, (3) accumulated opportunities, and (4) spatial analysis. A brief review follows.

(1) Network density. The network density of transportation facilities, such as bus stations, subway stations, and bus lines, can be used as an indicator of regional accessibility (Mavoa et al., 2012; Lu et al., 2016). The spatial distribution dimension of traffic networks can be used to represent the spatial connectivity and the spatial complexity (Lu and Tang, 2004; Lu et al., 2016). The city spaces are filled up more densely by traffic networks and the locations within a city are more accessible (Lu and Tang, 2004).

✉ Xiao-guang RUAN, ruanxg@zjweu.edu.cn
Xiao-guang RUAN, https://orcid.org/0000-0001-5017-0495

Received Sept. 6, 2021; Revision accepted Feb. 16, 2022;
Crosschecked June 30, 2022

(2) Spatial barriers. Space barriers may include distance costs, time costs, and expense costs (Salonen and Toivonen, 2013; Niedzielski and Boschmann, 2014). The weighted average travel time can reflect the spatio-temporal evolution of the accessibility in the transport network, but it cannot reflect the information on land use and transport demand (Rojas et al., 2016). It is also possible to establish a probabilistic model of travel time to estimate the travel time under different traffic conditions (Yildirimoglu and Geroliminis, 2013). With the average congestion delay model, regional delay estimates can be made (Mallinckrodt, 2010). On the basis of travel time costs and distance costs, the method of increasing the travel expense costs indicator can evaluate the equitable distribution of accessibility and transport planning more accurately (El-Geneidy et al., 2016; Martens and di Ciommo, 2017).

(3) Accumulated opportunities. Accumulated opportunities within the threshold range can be used to measure traffic accessibility, including resident population, job opportunities, and urban green space opportunities (Lyons and Urry, 2005; Metz, 2008). However, selecting the time threshold (such as 20 min) is sometimes difficult (Weiss et al., 2018).

(4) Spatial analysis. Using spatial analysis methods such as network theory, shortest path method, or gravity model, traffic accessibility can be quantitatively evaluated. The shortest travel time can be used to analyze road network evolution characteristics and accessibility characteristics (Koopmans et al., 2012; Farber and Fu, 2017). Geographic information system (GIS) spatial analysis has been used to establish a gravity model for quantitative analysis of road traffic accessibility pattern evolution (Kotavaara et al., 2012; Wan et al., 2012). The network model can determine the service coverage of public transport and then assess public transport accessibility at different levels (Saghapour et al., 2016). Based on the improved travel time and traffic network gravity model, the spatio-temporal distribution of urban green space accessibility can be analyzed (Ye et al., 2018).

However, actual traffic conditions are complex and an optimal travel plan is difficult to develop. The research on road traffic accessibility has limited geographical data. As the main data source for traffic location information, floating car data (FCD) can estimate and predict urban traffic states (Dewulf et al., 2015), but predictions are susceptible to vehicle penetration rates, data sampling frequencies, and vehicle coverage (Sanaullah et al., 2016; Rahmani et al., 2017; Shi et al., 2017). Several studies have shown that the data generated by social media, such as Foursquare users, combined with field survey data, can be used to study the commercial and social activity characteristics of urban networks (Agryzkov et al., 2012, 2014, 2017). Researchers have pointed out that openly available data sources and open path search interfaces based on web maps (such as the Journey Planner application programming interface (API)) can be used to analyze accessibility by applying spatial analysis models of multiple transportation modes (Niedzielski and Boschmann, 2014). With the open API interface, data such as travel time and travel distance between any two points in the city can be obtained (Hielkema and Hongisto, 2013). The Directions API, one of the Google Maps APIs, is a service that calculates directions between locations using a hyper text transport protocol (HTTP) request (Jäppinen et al., 2013).

To sum up, actual traffic conditions are complex, making it difficult to formulate an optimal travel plan, and the available geographical data for traffic accessibility research are limited. The objective of this study is to propose a method for analyzing the accessibility potential of urban road infrastructure based on the average travel speed during off-peak hours, and to rank the cities studied. On the one hand, the objective of this study is to understand whether it is feasible to supplement useful geographic data with Google Maps API network crawling technique, so as to obtain more practical and comparable results. On the other hand, we aim to demonstrate whether the average speed can be used as an indicator for measuring urban road traffic accessibility potential. With the aid of the Google Maps API web crawler, we obtain several sets of travel times and travel distances for several optimal routes from urban administrative districts and built-up areas to city centers. Then we calculate the average travel speed from urban administrative districts and built-up areas to city centers during off-peak times on working days. This work is carried out in 80 cities around worldwide. We then propose average travel speed in off-peak times as an indicator for evaluating the accessibility potential of urban road traffic.

The study is organized as follows. Section 1 summarizes the literature on accessibility analysis methods and evaluation indicators for transport infrastructure. Sections 2 and 3 give a detailed description of the data used and the processing methods. The results are analyzed in Section 4. Finally, Section 5 provides the conclusions.

2 Study area and data collection

The study areas comprised 80 cities worldwide from all six continents with rich terrain features, different scales, uniform location distribution, various economic strengths, and various urban forms. They include national capitals (e.g., Washington DC, London, Paris, Beijing, and Tokyo), economic centers (e.g., New York City, Los Angeles, and Shanghai), as well as developing cities (e.g., Rio de Janeiro and Johannesburg) (Fig. 5 in Section 4). The study was conducted with the object of investigating the spatial distribution characteristics of road accessibility potential in different types of cities and their respective directions that may need improvement. The data required for the study were in the following categories. The principle of the experiment is to ensure the consistency of data time as much as possible.

2.1 NPP-VIIRS night-time light data

Related research shows that according to the principle of its data acquisition, Suomi National Polar-Orbiting Partnership satellite's visible-infrared imaging radiometer suite (NPP-VIIRS) night-time light data have higher spatial resolution and wider radiation detection range. This avoids anomalous fluctuations in the digital number (DN) values of different satellites and different periods due to lack of flight calibration. Therefore, the accuracy of using NPP-VIIRS data to extract urban built-up areas is higher than that of the Defense Meteorological Satellite Program's Operational Linescan System (DMSP-OLS) night-time light data. In other words, NPP-VIIRS data can enable the extraction of urban built-up areas and the determination of city centers.

The night-time light grid data were downloaded from National Oceanic and Atmospheric Administration (NOAA), the USA with a resolution of 15″ (approximately 500 m) (https://www.ngdc.noaa.gov/eog/viirs/download_dnb_composites.html).

2.2 Landsat-8 OLI/TIRS image data

The medium spatial resolution remote sensing image can be used to verify the extent of urban built-up areas. On Feb. 11, 2013, NASA successfully launched the Landsat-8 satellite. The Operational Land Imager (OLI) can collect image data of nine shortwave spectral bands over a 185 km swath with a spatial resolution of 30 m for all bands except a 15 m panchromatic band (Irons et al., 2012). Landsat-8 OLI/TIRS images were downloaded from United States Geological Survey (USGS) (https://earthexplorer.usgs.gov/). According to the geographical characteristics of the study area, several Landsat-8 images were used as data for the study. To effectively identify and classify objects, the images in the study area should be guaranteed to have minimum cloudiness, be clear images, and be of good quality.

2.3 Administrative district data

Administrative boundary data, major river basins, and major roads are the main administrative district vector data required for research. They were downloaded from Resource and Environment Science and Data Center (RESDC), China (http://www.resdc.cn), OpenStreetMap (http://www.openstreetmap.org/), and DIVA-GIS (http://www.diva-gis.org/gData).

2.4 Socio-economic statistics

In addition, socio-economic statistics in cities can be used as supplementary and validation data. Annual built-up area statistics for some cities are published by the government. According to the definition of an urban built-up area in the Chinese City Yearbook, an urban built-up area is an area that has actually been developed and built in the administrative district, and municipal public facilities and other public facilities are available. The area statistics of China's urban built-up areas can be obtained from the China City Statistical Yearbook.

3 Methodology

The technical flow diagram of this study is shown in Fig. 1. It includes data preprocessing, selecting the starting points and the destinations, crawling the optimal route data (distance and time), and calculating the travel speed. The specific steps are as follows.

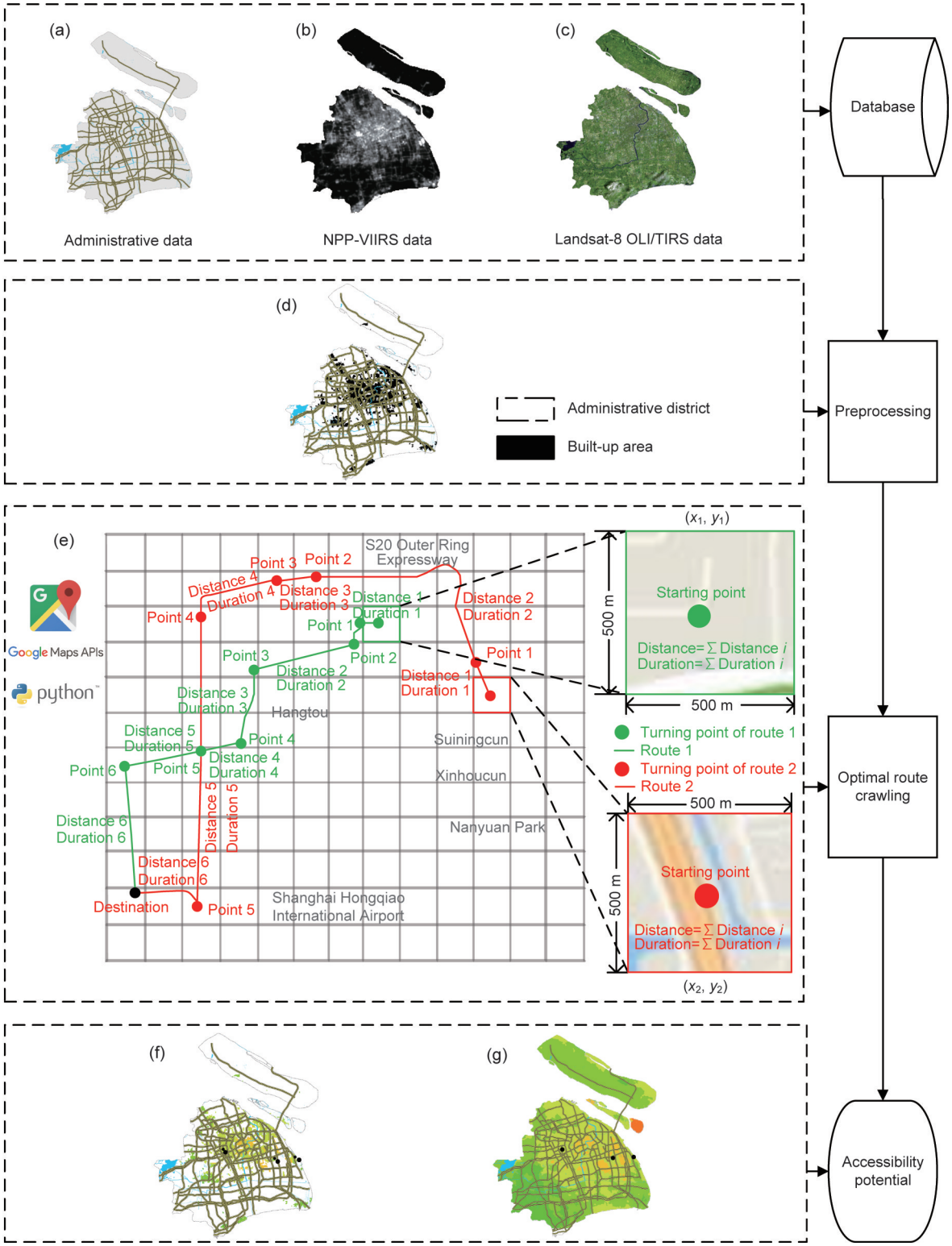

Fig. 1 Flow diagram of the study for the case of Shanghai, China: (a) administrative data; (b) NPP-VIIRS data; (c) Landsat-8 OLI/TIRS image; (d) built-up area; (e) two routes in Shanghai (each grid represents a starting point and the black circle represents the destination; the green line represents route 1 and the green circle represents its turning points; the red line represents route 2 and the red circle represents its turning points); (f) travel speed distribution in the built-up area; (g) travel speed distribution in the administrative district

3.1 Data preprocessing

To compare the differences in the accessibility potential of urban administrative districts and built-up areas and explain the level of urban development, it is necessary to extract built-up districts on the basis of administrative districts. The night-time light data of residential areas detected by NPP-VIIRS can effectively distinguish urban built-up areas and bare land (Zhang et al., 2014; Shi et al., 2016). The key issue is to find the threshold value of the light DN values. Of course, the different land cover types reflected by other remote sensing data, such as the Landsat series of satellite data, can also distinguish between urban and non-urban areas. However, due to the similarity between the built-up area and the surrounding land cover types (such as bare land), the accuracy of the extracted urban built-up area is limited (Zhang et al., 2002; Small and Lu, 2006).

Studies have found that the accuracy of the statistical-assisted thresholding method is the highest by comparing several commonly used built-up area extraction methods, and the method is a widely used method for extracting urban built-up areas (Imhoff et al., 1997; Ma et al., 2012). Annual statistics on the built-up areas of Chinese cities are published by the government, and they are easily available. These data can be used as auxiliary data, such as the Chinese City Yearbook (Shi et al., 2016; Chen ZQ et al., 2017). By setting different thresholds for the light image, the obtained built-up area range is compared with the urban range in the reference image (Imhoff et al., 1997). The light data threshold value when the built-up area range is the closest to the reference image is taken as the optimal threshold value. Spatial comparisons of higher resolution image data can be used to take into account the spatial distribution characteristics of built-up areas (Zhou et al., 2014). In this paper, for Chinese cities with statistical data of urban built-up areas, the statistical-assisted thresholding method was used to extract built-up areas based on NPP-VIIRS data. For other cities, without statistics of urban built-up areas, the empirical thresholding method was used to extract built-up areas based on NPP-VIIRS data. The results were verified by visual interpretation of Landsat-8 OLI/TIRS images (dotted line shown in Fig. 2). The visual interpretation of remote sensing images can obtain the necessary geothematic information from remote sensing images, interpret their distribution, and give rough estimates of their quantitative characteristics (Zha et al., 2003). The details of the method are as follows (Fig. 2). When the grids in the building area extracted by NPP-VIIRS data are equal to those according to the statistical yearbook, the threshold that constitutes the built-up area can be determined and the built area can be calculated.

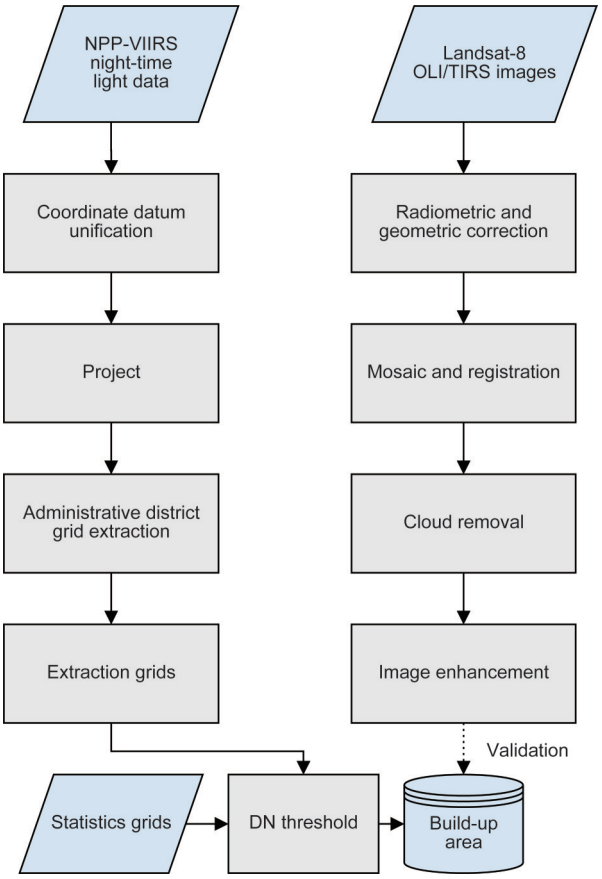

Fig. 2 Flow chart of extracting urban built-up area (the dotted line represents validation)

First, we preprocessed the 2015 NPP-VIIRS night-time light data. We used the administrative district as a mask to extract the 15″ grids of the study area and projected and registered it into a unified geographic reference system. In addition, because Canberra (the capital of Australia) and the city-state of Monaco are very small, it was not necessary to use a 500 m×500 m grid for analysis. In these cases, the grid data were resampled to a size of 50 m for analysis. In the study, all raster and vector data were projected into the WGS 1984 Web Mercator Auxiliary

Sphere projection system with the World Geodetic System datum (WGS-84) and a basic information database was established.

Next, we used the ENVI application software to preprocess the original Landsat-8 OLI/TIRS images, including radiometric and geometric corrections, image mosaic, image registration, and cloud removal. The error was controlled within one pixel, and the remote sensing image range of the study area was extracted by the city administrative vector boundary. Image enhancements and fusions are required to ensure visual interpretation. Band 7, band 6, and band 4 in spectral bands of Landsat-8 OLI/TIRS images were combined to obtain natural-color composite images. With the help of this composite image, naked land and cities can be distinguished.

Finally, for Chinese cities that have annual built-up area statistics released by the government, we first set a dynamic threshold based on the distribution of the DN value corresponding to the study area and calculated the total area of all pixels larger than the threshold. Then, by constantly changing the threshold size, we compared the area and statistical data of the urban built-up area under each threshold. When their absolute difference reached a minimum, the corresponding DN value was considered as the optimal threshold. We used this threshold to extract built-up areas. According to the imaging differences in built-up areas and non-built-up areas in the Landsat-8 OLI/TIRS images, the boundary and spatial distribution of the built-up areas were visually interpreted to verify their reliability. For other cities without accurate statistics of built-up areas, we first referred to the thresholds obtained in the previous step to estimate the empirical thresholds. The principle was that the city to be referenced and the city to be determined had the same scale, similar form, and close DN value range. Then, the extracted built-up area range was verified by the built-up area range visually interpreted by Landsat-8 OLI/TIRS images. Finally, appropriate adjustments were made to obtain a more accurate built-up area. Finally, appropriate adjustments were made, that is, the DN value was changed to obtain a more accurate built-up area.

The optimal DN value thresholds for the extraction of built-up areas in some cities are shown in Table 1.

3.2 Selecting the starting points and the destinations

3.2.1 Selecting the starting points

To examine the urban road accessibility potential using more realistic and accurate urban travel speeds, it is necessary to extract the travel routes between starting points and destinations of different locations in the urban area. In this study, we make regular grids of cities and use the grids as starting points for the routes. The details of the method are as follows.

First, according to the method described in Section 3.1, 80 study areas were preprocessed to obtain the corresponding urban administrative districts and urban built-up areas. Then, the 15″ (about 500 m× 500 m, excluding Canberra and Monaco) grids of the NPP-VIIRS night-time light data in the urban administrative districts and urban built-up areas were

Table 1 Optimal DN value thresholds of 11 cities in China

City	Grid number in administrative district	Threshold of NPP-VIIRS (nW/(cm^2·sr))	Built-up area* (km^2)
Shanghai	37069	36.61	1400
Beijing	99765	20.99	1597
Tianjin	70388	26.14	902
Chengdu	58879	27.82	604
Wuhan	45401	23.25	506
Nanjing	36195	19.12	735
Nanchang	39327	14.22	268
Yinchuan	42748	31.81	167
Zhenjiang	21048	22.58	138
Ma’anshan	9781	20.33	90
Suihua	18635	31.45	27

* The urban built-up areas are obtained from China City Statistical Yearbook (NBSC, 2016)

converted into points, i.e., the geometric center point of each pixel of the raster dataset was used as a starting point (Fig. 1). Finally, we calculated the geographic coordinates of all starting points consistent with Google Maps and exported point dataset for crawling routes. The numbers of starting points in different cities differed as the cities varied in size. The numbers of starting points in some cities are shown in Table 1.

3.2.2 Selecting the destinations

According to existing research, DMSP-OLS or NPP-VIIRS data can reflect the spatial distribution of socio-economic characteristics. Human activity is positively correlated with DN values of night-time light imagery (Langford et al., 2008; Shi et al., 2016). We conducted this study with the object of investigating the accessibility potential of all grids to the city centers. Therefore, the NPP-VIIRS data from 2015 were used to determine the city centers. Excluding high DN values such as oil refineries, oil storages, ports, and highway intersections, several candidate city centers were determined by referencing the existing localized contour tree method (Chen ZQ et al., 2017). The principle of this method is based on the similarity of urban structure and topography. This method generates a contour map from NPP-VIIRS data, constructs a DN value contour tree, and finally identifies element city centers as leaf node of the contour tree. It has many advantages, including the ability to accurately depict the spatial extent of the city center and determine the hierarchical spatial relationship between urban centers at different scales (Chen ZQ et al., 2017). Using the localized contour tree method, we successfully identified several centers in 80 cities. Then, the results were verified by Google Earth software.

It should be noted that the main purpose of this study is to achieve intra-city accessibility potential. In other words, the type of destination is not important, and the distribution is the main basis for selection. We define urban centers as parts of the city where human activity is highly concentrated (Couturier et al., 2011). To consider the different types of travel activities, including work, travel, sports activities, leisure activities, and religious activities, we identified such centers that were mainly located in commercial centers, urban transportation hubs (e.g., central stations), sports and leisure venues, etc., and then used them as the destinations. The center points of some cities are shown in Table 2.

3.2.3 Crawling route data (distance and time)

Google Maps predicts the results and actual time through historical data in a certain area. The data includes local speed limit and recommended speed, different road speeds, historical average speed at a certain time, actual time spent by other users, and real-time traffic conditions. The algorithm and database are adjusted over time (Wang and Xu, 2011). The principle of the Google Maps is to design the best driving plan according to the specified travel mode based on the attributes of the routes between the starting points and the destinations. Then, according to the rules of the shortest time or the shortest route, it calculates and returns the average travel time and average travel distance of each route. With the Directions API, we can crawl directions for several modes of transportation, including transit, driving, walking or cycling. The operation mechanism of public transportation is complicated, and the travel plan may not be accurate enough. Therefore, the chosen mode of travel used in this study was driving. When the Directions API returns results, it places them within a route array (Wang and Xu, 2011). Even if the service returns no results (e.g., the origin and/or destination does not exist), it still returns an empty route array.

Take Shanghai's planning route from each starting point to Hongqiao Railway Station as an example (Fig. 1). The Google Maps API reads the latitude and longitude coordinates of the starting points and the destination, and plans the best travel route under the driving mode (travel mode), including the position of each turning point, the distance of each section in the route, the duration of each section in the route, road names, and driving behaviors or strategies (including "continue straight", "turn-left", "turn-right", and other information). The default settings include the travel mode of driving, and the route does not avoid the expressway, does not avoid the toll station, and does not avoid the ferry. The distance unit was set to meter, and the time unit was set to second. For requests where the travel mode is driving, the user can specify the desired time of departure. You can specify the time as an integer in seconds since midnight, Jan. 1, 1970 UTC (universal time coordinated). It should

Table 2 Centers in some cities in this study

City	Centers	Longitude	Latitude
Buenos Aires	May Square	58.3723°W	34.6084°S
	Rose Garden	58.4176°W	34.5704°S
Cape Town	Cape Town International Airport	18.5963°E	33.9703°S
	Cape Town International Convention Center	18.4280°E	33.9163°S
Los Angeles	Port of Los Angeles	118.2525°W	33.7333°N
	Hollywood/Vine Station	118.3259°W	34.1012°N
	Los Angeles International Airport	118.4041°W	33.9461°N
	Staples Center	118.2668°W	34.0430°N
Istanbul	Hagia Sophia	28.9796°E	41.0087°N
	Atatürk Havalimanı	28.8193°E	40.9799°N
Madrid	Santiago Bernabéu Stadium	3.6883°W	40.4531°N
Moscow	Revolution Square	37.6213°E	55.7566°N
	Spartak Stadium	37.4407°E	55.8178°N
New York City	Times Square	73.9877°W	40.7582°N
	Kennedy International Airport	73.7836°W	40.6461°N
Paris	The Louvre	2.3342°E	48.8614°N
	The Princes' Park Stadium	2.2530°E	48.8416°N
Phnom Penh	Phnom Penh International Airport	104.8447°E	11.5529°N
	3G Sport Center	104.9340°E	11.5532°N
	National University of Management	104.9188°E	11.5742°N
Shanghai	Shanghai Hongqiao Railway Station	121.3271°E	31.2006°N
	Shanghai Pudong International Airport	121.8132°E	31.1558°N
Tokyo	Tokyo Station	139.7660°E	35.6814°N
	Tokyo's Ginza District	139.7644°E	35.6715°N

be pointed out that our aim is not to compare the traffic conditions of different time periods (such as peak hours and off-peak hours) in the same city, but to compare the similarities and differences between different cities by using the proposed method framework (Fig. 1). In this study, it is necessary to select the same time period to control the interference caused by different times, so we set the departure time to 10:00 PM on the local time workday. Some fields used in the process of crawling one route in Shanghai are shown in Table 3, and some results obtained.

Table 3 Some fields used in the process of crawling route data

Field	Result
End address	Qixin Road, Minhang District, Shanghai, China
End location	Latitude: 31.2006°N; longitude: 121.3271°E
Start address	Weiqi Road, Baoshan District, Shanghai, China
Start location	Latitude: 31.4880°N, longitude: 121.4935°E
Turning point	Latitude: 31.3775°N, longitude: 121.4980°E
Maneuver	Turn-right
Departure time	1526608800 (May 18, 2018 at 10:00 PM)
Travel mode	Driving
Distance	0.6 km (554 m)
Duration	2 min (90 s)

3.2.4 Calculating the speed

To analyze the distribution of road accessibility potential within each city, we introduced the average travel speed of each route (S_{Avg}) in an urban administrative district and built-up area during off-peak times. According to the method described in Section 3.1, all travel routes from the starting points (500 m×500 m grid points in urban administrative districts and built-up areas) to the city centers can be crawled by the Google Maps API. The algorithm judges the location information of the user-defined starting point and determines whether it is located on the road network. According to the road attribute information, Google Maps API defines the road network as various grades of roads that can be driven. If the starting point is not located on the road network, the point coordinates on

the road closest to the starting point of the route are calculated as the starting point for the road network reachability analysis. Each route contains the position of each turning point, the distance of each section in the route, and the duration (the travel time) of each section in the route. The time and distance of the routes crawled by the Google Maps API are the basic data, and the average travel speed between the starting point and the center point of each route is calculated as follows:

$$D_{\text{route}} = \sum \text{Distance } i, \tag{1}$$

$$T_{\text{route}} = \sum \text{Duration } i, \tag{2}$$

$$S_{\text{Avg}} = \frac{D_{\text{route}}}{T_{\text{route}}}, \tag{3}$$

where D_{route} represents the travel distance of one route, T_{route} represents the travel time of one route, "Distance i" represents the distance of each section in the route, and "Duration i" represents the travel time of each section in the route.

To compare and rank the accessibility potential of 80 cities, we introduced the average travel speed in the entire city during off-peak times, including the average travel speed in administrative district (A) and in built-up area (B). The former refers to the average travel speed from all the starting points in the urban administrative area to city centers during off-peak hours. The latter refers to the average travel speed from all the starting points in the urban built-up area to city centers during off-peak hours.

In the previous step, we have calculated the T_{route}, D_{route}, and S_{Avg} of all routes. Then, the average travel speed of all routes in the entire city range is calculated according to the linear least squares (Fig. 3). Where the horizontal axis represents T_{route} and the vertical axis represents D_{route}, and the linear coefficient represents the average travel speed in the entire city.

4 Results and discussion

This study used S_{Avg} as an indicator to measure and analyze the differences in accessibility potential within cities. In addition, we explored the road accessibility potential of a city from two aspects, A and B during off-peak times.

4.1 Accessibility potential within the representative cities

Globalization and World Cities (GaWC, 2016) divides most of the world's cities into several levels according to their degree of connection with the world in economic globalization: namely, α, β, γ, and cities with sufficiency of services (Taylor, 2001). According to the classification criteria of GaWC, we selected 17 representative cities and compared the spatial differences in their accessibility potential (Fig. 4). To verify whether the average travel speed of the vehicle can directly reflect the road accessibility potential within the city in which it travels, the S_{Avg} within the 17 cities was divided into six intervals of [0, 30],

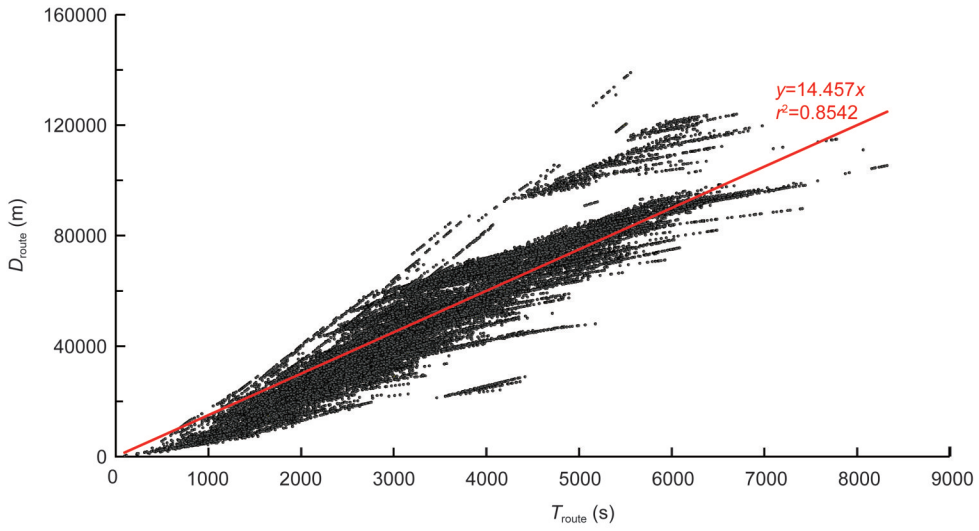

Fig. 3 Average travel speed calculation result, i.e., relationship between D_{route} and T_{route}

(30, 40], (40, 50], (50, 60], (60, 70], and (70, 90], where the unit was km/h. The main expressways, highways or major ways in the cities were also illustrated in Fig. 4. The representative cities were divided into three categories as described below.

Among the 17 cities, the average travel speed in administrative district (*A*) and the average travel speed in built-up areas (*B*) of Cape Town, Los Angeles, and Shanghai are all above 50 km/h. In this study, they are among the largest cities on their respective continents, with multiple city centers. In their central area, the roads are densely distributed, but the S_{Avg} is roughly between (40, 50] and (50, 60] (km/h). The S_{Avg} gradually increases from the center circle to the peripheries of these cities and is evenly distributed. The S_{Avg} in almost all areas is above 50 km/h and the maximum S_{Avg} can reach above 70 km/h. In addition, in their areas far from the central area, the S_{Avg} of areas with high-grade roads is larger than that of areas without high-grade roads, but the difference is not obvious. Cape Town (Fig. 4a-1), the second largest metropolis and the legislative capital of the Republic of South Africa, is home to the parliament and numerous government agencies (Magruder, 2010). Its average travel speed in the urban administrative district (*A*) and average travel speed in urban built-up areas (*B*) are 63.84 km/h and 60.87 km/h, respectively. Cape Town is the starting point of three major highways in the west of South Africa, including the N1 (national highway), N2, and N7. The N1 and N2 roads start at the northern end of Buitengracht Street (near one city center selected in this study, CTICC) and split into two at the eastern end of the Central Business District. N1 extends to the northeast of the city, whereas N2 runs southeast through Cape Town International Airport (another city center). Cape Town, like most South African cities, uses metropolitan or "M" routes for important intra-city routes, a layer below national (N) roads and regional (R) roads. Each city's M roads are independently numbered. These roads interact with Cape Town's N and R roads. Los Angeles (Fig. 4d-1) has a complex multimodal transport system that serves as a hub for regional, domestic, and international passenger and freight transport. There are more than a dozen major expressways across the city, including Harbor Freeway (I-110) and Santa Monica Highway/San Bernardino Expressway (I-10). The city has an extensive street grid. Arterial streets connect expressways to smaller streets and are often used to bypass crowded expressway routes. In Los Angeles, *A* and *B* are 62.69 km/h and 61.26 km/h, respectively. Shanghai (Fig. 4b-1), one of the four direct-controlled municipalities of China and the most populous cities in the world, has *A* and *B* respectively of 62.31 km/h and 57.72 km/h. Most of the municipal highways in Shanghai are in inland areas. These roads are called urban expressways in Chinese. These roads generally have ramps, sections, and grades, and there are no traffic lights. Their maximum speed is 80 km/h; further, they form an inner loop. The national highway G40 connects Chongming Island and Changxing Island. As a result, the accessibility potential in these two regions is better.

Among the 17 cities, *A* and *B* of New York City, Gaborone, Santiago, Kuala Lumpur, Istanbul, Moscow, Brasilia, and Wellington are mostly between 30 km/h and 50 km/h. They have a single center or multiple city centers. In the central area where the city center is located, the S_{Avg} is basically lower than 30 km/h. The S_{Avg} gradually increases from the center circle to the peripheries of these cities, but the distribution is uneven. The maximum S_{Avg} is below 60 km/h, except for parts of New York City and Santiago. In areas far from the central area, the S_{Avg} of areas with high-grade roads is larger than that of areas without high-grade roads, and the difference is very obvious, and the S_{Avg} on both sides of the road is large, especially in New York City, Gaborone, Santiago, and Moscow. In all seven cities, more than 50% of the regions have the S_{Avg} below 40 km/h. Gaborone (Fig. 4a-2), the capital city of Botswana, has *A* and *B* respectively of 38.20 km/h and 35.00 km/h. The A1 is the main highway connecting Gaborone and its surroundings.

There are five major roads in Gaborone that go to Lobatse, Kanye, Molepolole, Francistown, and Tlokweng. New York City (Fig. 4d-2) is the most populous city in the United States, and *A* and *B* in New York City are 47.54 km/h and 45.92 km/h, respectively. The transportation system of New York City is a network of complex infrastructural systems. Although New York City relies on public transportation, roads are an important feature of the city. In Manhattan, there are 12 numbered avenues parallel to the Hudson River, and 220 numbered streets perpendicular to the river. The city's extensive expressway network

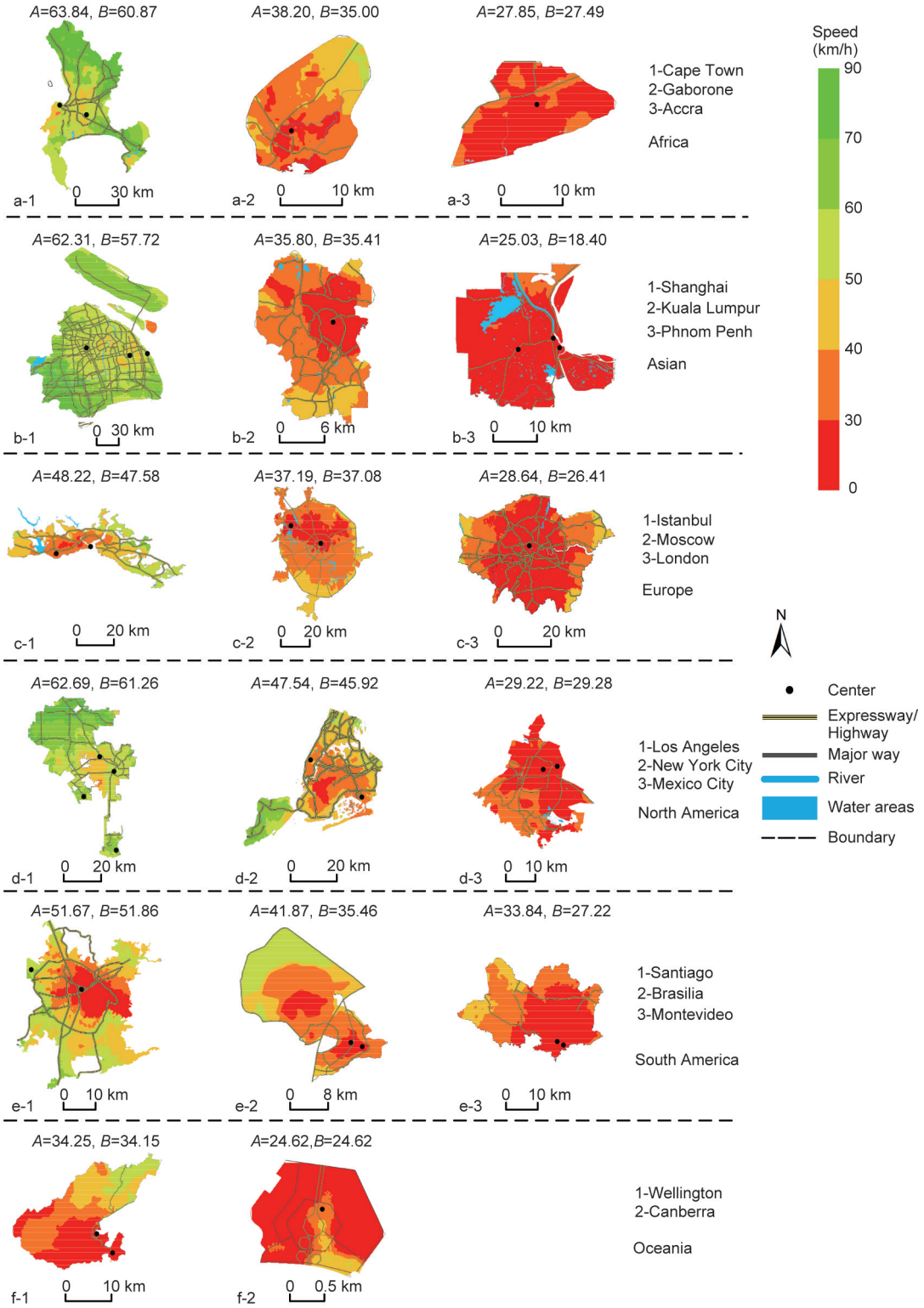

Fig. 4 Travel speed distribution in representative cities (unit: km/h). According to GaWC, London and New York City are classified as α++; Shanghai is classified as α+; Kuala Lumpur, Los Angeles, Istanbul, Mexico City, and Moscow are classified as α; Santiago is classified as α−; Cape Town is classified as β+; Montevideo is classified as β; Accra is classified as γ; Gaborone and Wellington are classified as γ−; Phnom Penh is classified as high sufficiency; Brasilia and Canberra are classified as sufficiency

includes six major interstate highways and four major state highways. Wellington (Fig. 4f-1) is the capital of New Zealand and the southernmost capital in the world. As one of New Zealand's major ports and a transportation hub between the North Island and the South Island, its A and B are 34.25 km/h and 34.15 km/h, respectively. Because of the severe limitations of mountain terrain, Wellington is served by SH 1 (State Highway 1) and SH 2 (State Highway 2), which meet at Ngauranga, north of the city center. The Urban Motorway, part of SH 1, is the major road into and out of Wellington and extends from the base of the Ngauranga Gorge into the Wellington central business district (CBD).

Among the 17 cities, A and B of Accra, Phnom Penh, London, Mexico City, Montevideo, and Canberra are all below 30 km/h, except for Montevideo (A= 33.84 km/h). They are generally small, and the urban center circles are not obvious. The S_{Avg} does not increase significantly from the center circle to the peripheries of these cities, and the maximum S_{Avg} is below 50 km/h. There is basically no difference in the S_{Avg} of areas with high-grade roads and that of areas without high-grade roads. In all six cities, the S_{Avg} is below 30 km/h in almost all areas. Accra (Fig. 4a-3), the capital city of Ghana, has A and B respectively of 27.85 km/h and 27.49 km/h. The N1, spanning more than 500 km across Ghana, is an important corridor connecting several countries in West Africa. It links Kotoka International Airport and two important ports in Ghana, where Kotoka International Airport is considered to be the city center of Accra (Noora et al., 2016). Phnom Penh (Fig. 4b-3), the capital and the most populous city of Cambodia, is located on the banks of the Tonle Sap River and the Mekong River. It is connected to the rest of the country through the national roads as well as by domestic flights to and from Phnom Penh International Airport (one of the city centers). Warfare seriously damaged Cambodia's transportation system and it was not until 2006 that most of the roads began to improve and major highways were gradually upgraded to international standards. In Phnom Penh, A and B are 25.03 km/h and 18.40 km/h, respectively.

4.2 Ranking of road accessibility potential

To compare and rank the accessibility potential of 80 cities, the average travel speeds in the entire city were divided into three intervals of (0, 30], (30, 50], and (50, +∞), where the unit was km/h. Figs. 5 and 6 illustrate the results of sorting 80 cities according to their average travel speeds.

In all 80 cities in the study area from all six continents in the study area (Fig. 5), the mean average travel speed in the urban administrative district (A) is 37.22 km/h. There are 27 cities with speed lower than 30 km/h, 41 cities with speed ranging from 30 km/h to 50 km/h, and 12 cities with speed higher than 50 km/h. Among them, Ottawa has the highest speed, reaching 71.03 km/h, and the city with the lowest average speed is Lima (14.77 km/h).

In the study area (Fig. 6), the mean average travel speed in the urban built-up areas (B) is 34.00 km/h, of which Los Angeles has the highest speed, reaching 61.26 km/h. Lima and the City of Monaco are the two smallest cities in size. Their urban administrative district is equal to the urban built-up area. The average speeds of the two urban built-up areas are the lowest,

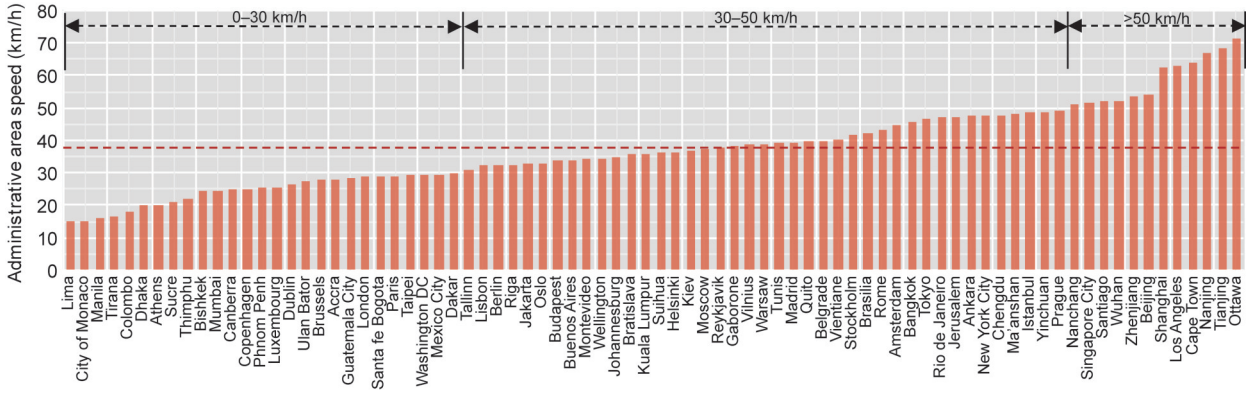

Fig. 5 Average travel speed statistics in the urban administrative district for 80 cities around the world. The dashed line refers to the mean average travel speed in the urban administrative district (A)

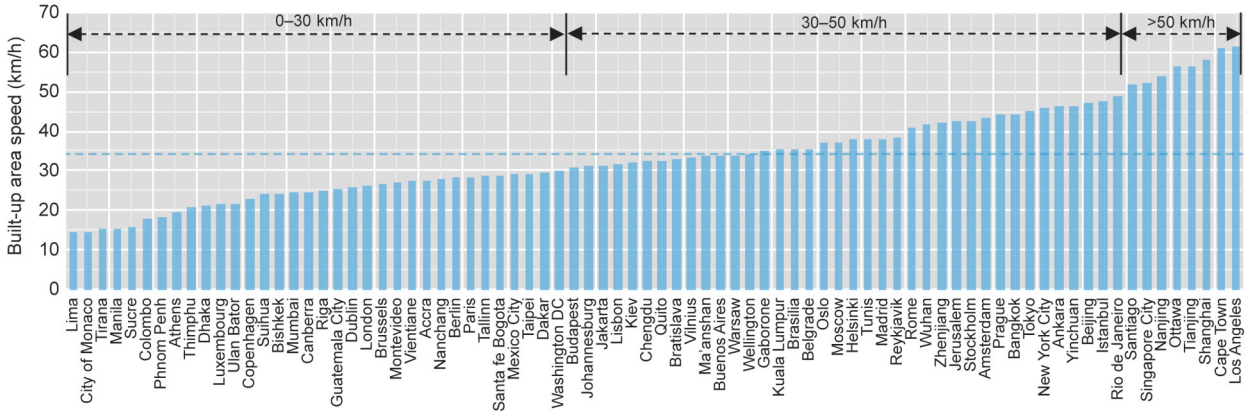

Fig. 6 Average travel speed statistics in the urbant built-up areas for 80 cities around the world. The dashed line refers to the mean average travel speed in the urban built-up areas (*B*)

at 14.77 km/h and 14.78 km/h, respectively. There are 34 cities with speed lower than 30 km/h, 38 cities with speed in the range of 30–50 km/h, and eight cities with speed higher than 50 km/h.

To compare and analyze the difference between A and B, another indicator is introduced, namely, $S_{A\text{-}B}$, which refers to the difference between A and B. $S_{A\text{-}B}>0$ means that A is higher than B, $S_{A\text{-}B}=0$ means that A is equal to B, and $S_{A\text{-}B}<0$ means that A is lower than B. There are 61 cities with $S_{A\text{-}B}>0$, accounting for about 75% of all research areas, including all cities in China except Taipei. In such cities, the built-up area is generally smaller than its administrative area. The vehicle flow in their central or built-up areas is larger and the speed is lower than in their administrative districts (Figs. 4–6). The cities of Monaco, Canberra, and Lima have $S_{A\text{-}B}=0$, that is, A is equal to B (Figs. 5 and 6). The size of such cities is generally small, and the entire city is the built-up area. In addition, the remaining 16 cities have $S_{A\text{-}B}<0$. The maximum difference is Oslo, at only −4.49 km/h. In such cities, B is slightly higher than A (Figs. 5 and 6), which may be because the carrying capacity of the road network can meet the vehicle flow. This means that although B is less than A in most cities, $S_{A\text{-}B}$ in more than half of the cities (43 in total) is within [−2, 2] (km/h).

4.3 Distribution characteristics of accessibility potential

The overall accessibility potential distribution of these cities in Sections 4.1 and 4.2 has two characteristics. First, the average travel speed near the city centers is generally lower than that of the peripheries. Within the coverage of the expressway, the farther away from the center of the city, the higher the travel speed. Second, the travel speed is in fact the same along the same level of the road. In areas where the distance to the city center is almost equal, the closer to the expressway, the higher the travel speed. The more expressway distribution along the route, the higher the speed of travel. The reasons for these characteristics are as follows.

The route from one starting point has a different speed in each section of the route. The speed of the low-grade section near the city center is low, whereas the speed of the high-grade section in the peripheries is high. This is because of a combination of factors such as the design speed of each section of the route and the vehicle flow (Shirgaokar, 2014). A phenomenon has been formed in which the speed of some sections is very low, but the average speed of the entire route is not low, while the speed of some sections is high, but the average speed of the entire route is not high.

When a route is planned, Google Maps gives priority to the highest-grade road that can be reached. Fig. 7 illustrates three routes from the three starting points in the city of Madrid, Spain to the Santiago Bernabéu Stadium. The red, blue, and green dots represent three starting points, and the black dot represents the destination. The black-red solid line represents the route 1, the black-blue solid line represents the route 2, and the black-green solid line represents the route 3. The figure also highlights the high-grade roads. In the first half, route 1 is along E-5, route 2 is along M-21, route 3 is along A-2, and finally the three routes meet at the intersection of E-5 and A-2. Then,

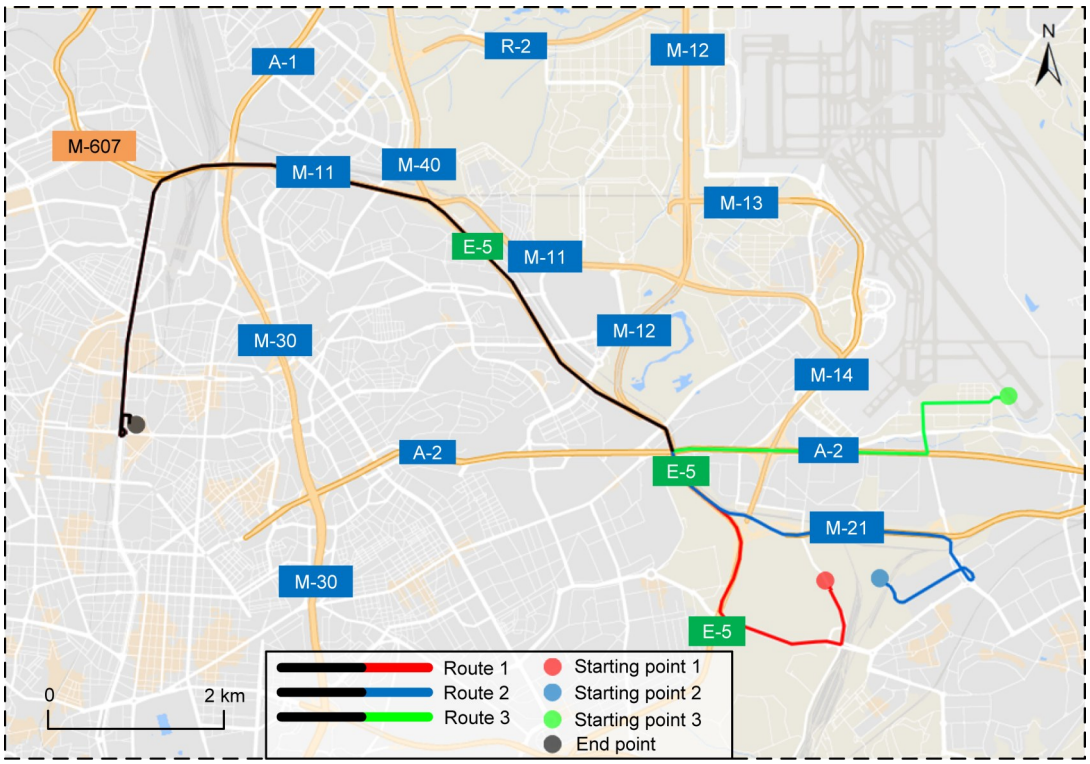

Fig. 7 Various routes to the city center of Madrid, Spain

all three are along E-5 and M-11 and reach the end point. That is, the route of the latter half is the same. The formation of a route is similar to the spatial distribution of water systems in river basins. That is, low-level routes will continue to be routed to higher-level routes through data comparisons, virtually increasing the overall operating efficiency of the city. Of course, higher-grade roads mean faster speed and convenience. The ability to connect different grades of roads can also reflect the accessibility potential of a city's road traffic (Cheng and Chen, 2015).

4.4 Usefulness and limitations of methods and indicators

As described in Section 4.3, the speed indicator in this paper reflects both the time attribute and the distance attribute of the optimal planning route, which can be used as an intuitive indicator to measure the traffic conditions in a city. In addition, several studies assert that the two important causes of urban road traffic congestion are the low density of urban roads and the inability to meet people's travel needs (Levine and Garb, 2002; Su, 2011). This study demonstrates that although there are main expressways, highways, or high-grade roads in the central area of the city, the vehicle flow is large, which leads to exceeding the carrying capacity of the road network. As a result, the speed is low, that is, the accessibility potential is poor. For non-urban central areas, in areas with main expressways, highways or high-grade roads, the carrying capacity of the road network can meet people's travel needs, the speed is high, and the accessibility potential is good. Furthermore, in the area where the urban trunk or branch road is concentrated, because the vehicle flow also exceeds the carrying capacity of the road network, the speed is low and the accessibility potential is poor. In other urban areas than the above, mainly due to the low level of roads, the lack of road network results in poor accessibility potential. It can be seen that the speed of each region is consistent with its corresponding road infrastructure level, the vehicles flow or regional development level (Birr et al., 2014), which indicates that the selected indicators can effectively determine the spatial differentiation of road accessibility potential.

Due to the shortcomings of the web map data itself and the influence of multiple factors of road traffic conditions, it was difficult to simulate the most realistic geographic scene (Wang and Xu, 2011). Road

conditions may vary from hour to hour, day to week. As a result, there are significant differences in the results at different times of the day. The accessibility characteristics in different scenarios should be a key point in future study, e.g., accessibility in rainy, snowy or sunny days, in winter or summer, on work week or vacation time, and even under temporary traffic control or not. Multi-source data fusion for spatial analysis has become a trend. Further research is needed to integrate real-time travel trajectory data (such as GPS floating car data and bus station data) and induction loop data (Geroliminis and Sun, 2011) in cities, so as to enhance the quality of traffic information, express the city's traffic conditions, conduct traffic analysis, and detect defective urban planning and areas with outstanding traffic problems.

4.5 Main possible policy implications

The possible policy implications from our study are as follows. Different cities have different traffic conditions, and the relationships between the spatial distribution of different types of cities and the traffic accessibility potential are not the same. Different types of cities should use different measures to improve road accessibility potential and achieve reasonable transportation planning. For cities such as Phnom Penh, Thimphu, Dhaka, Accra, Mumbai, Vientiane, and Jerusalem, which have a decentralized development model, it is particularly important to improve the road accessibility potential to change the situation of slow urbanization. Cities of this type can improve their road infrastructure by increasing road density, optimizing road locations (Atkinson et al., 2005), and changing the location of existing routes (Weber, 2018). Studies have found that in certain circumstances (Taylor et al., 2000; Šenk and Ambros, 2011), the faster the speed, the higher the frequency of traffic accidents. In these cities, the level of road transportation should be improved, such as improving the technical level of speed monitoring, and formulating and implementing traffic regulations. Cities with limited land space, such as London, Tokyo, Singapore, Jakarta, Kuala Lumpur, Bangkok, and Mexico City, have limited urban built-up areas, with no ability to significantly increase road density. In such cities, if new roads are built blindly, their contribution to accessibility potential may be limited. The following measures may make more sense: appropriately upgrading existing roads (broadening, maintaining, etc.), adding high-grade roads in congestion-prone areas, increasing the level of communication between high-grade roads, and developing underground tunnels. The disadvantages of blindly building inner loop roads have been proved, the isolation of road network systems and the increase in travel distance will undoubtedly increase travel costs (Ge and Gao, 2008). Constructing inner loop roads to alleviate traffic congestion is not a good choice. If the location of the city center (i.e., the gathering place of residents) is fully considered in the traffic planning, the construction and optimization of high-grade roads linking multiple city centers can solve the above problems to some extent. The development of urban public transport based on urban light rail, rail transit, elevated railways, etc., to achieve 3D urban travel and fully utilizing the existing urban structure and traffic layout, is the main direction of traffic planning for most cities.

5 Conclusions

This study examined the road accessibility potential in cities using more realistic and accurate measures of travel speed and delineation of urbanized area. Using the Google Maps API network crawling technique, it is feasible to crawl the optimal route to city centers. The average travel speed difference between 80 cities from six continents during off-peak times was calculated, including the average travel speed from the urban administrative district and urban built-up areas. The main conclusions are as follows:

1. The mean average travel speed in the urban administrative district (A) is 37.22 km/h, the mean average travel speed in the urban built-up areas (B) is 34.00 km/h. The speed is consistent with the road infrastructure level, the vehicle flow, and regional development level.

2. The results show that the selected indicators can effectively determine the spatial differentiation of road accessibility potential. The travel time and travel distance obtained by the proposed method can be used as the geographic data for the analysis of urban roads. Urban areas with high speed have good accessibility potential, whereas areas with low speed have poor accessibility potential.

3. This method offers a new possibility of analyzing traffic accessibility using internet data and geo-spatial methods. It may be able to quantitatively analyze issues in transport geography. The city speed results and rankings might serve as an international dataset.

Acknowledgments

This work is supported by the Zhejiang Provincial Natural Science Foundation of China (No. LZJWY22E090002) and the Zhejiang Provincial Water Conservancy Science and Technology Plan Project (No. RC2141), China.

References

Agryzkov T, Oliver JL, Tortosa L, et al., 2012. An algorithm for ranking the nodes of an urban network based on the concept of PageRank vector. *Applied Mathematics and Computation*, 219(4):2186-2193. https://doi.org/10.1016/j.amc.2012.08.064

Agryzkov T, Oliver JL, Tortosa L, et al., 2014. Analyzing the commercial activities of a street network by ranking their nodes: a case study in Murcia, Spain. *International Journal of Geographical Information Science*, 28(3):479-495. https://doi.org/10.1080/13658816.2013.854370

Agryzkov T, Martí P, Tortosa L, et al., 2017. Measuring urban activities using foursquare data and network analysis: a case study of Murcia (Spain). *International Journal of Geographical Information Science*, 31(1):100-121. https://doi.org/10.1080/13658816.2016.1188931

Atkinson DM, Deadman P, Dudycha D, et al., 2005. Multi-criteria evaluation and least cost path analysis for an arctic all-weather road. *Applied Geography*, 25(4):287-307. https://doi.org/10.1016/j.apgeog.2005.08.001

Birr K, Jamroz K, Kustra W, 2014. Travel time of public transport vehicles estimation. *Transportation Research Procedia*, 3:359-365. https://doi.org/10.1016/j.trpro.2014.10.016

Bowen J, 2000. Airline hubs in Southeast Asia: national economic development and nodal accessibility. *Journal of Transport Geography*, 8(1):25-41. https://doi.org/10.1016/S0966-6923(99)00030-7

Chen J, Ni JH, Xi CB, et al., 2017. Determining intra-urban spatial accessibility disparities in multimodal public transport networks. *Journal of Transport Geography*, 65:123-133. https://doi.org/10.1016/j.jtrangeo.2017.10.015

Chen ZQ, Yu BL, Song W, et al., 2017. A new approach for detecting urban centers and their spatial structure with nighttime light remote sensing. *IEEE Transactions on Geoscience and Remote Sensing*, 55(11):6305-6319. https://doi.org/10.1109/TGRS.2017.2725917

Cheng YH, Chen SY, 2015. Perceived accessibility, mobility, and connectivity of public transportation systems. *Transportation Research Part A: Policy and Practice*, 77:386-403. https://doi.org/10.1016/j.tra.2015.05.003

Couturier S, Ricárdez M, Osorno J, et al., 2011. Morpho-spatial extraction of urban nuclei in diffusely urbanized metropolitan areas. *Landscape and Urban Planning*, 101(4):338-348. https://doi.org/10.1016/j.landurbplan.2011.02.039

Démurger S, 2001. Infrastructure development and economic growth: an explanation for regional disparities in China? *Journal of Comparative Economics*, 29(1):95-117. https://doi.org/10.1006/jcec.2000.1693

Dewulf B, Neutens T, Vanlommel M, et al., 2015. Examining commuting patterns using floating car data and circular statistics: exploring the use of new methods and visualizations to study travel times. *Journal of Transport Geography*, 48:41-51. https://doi.org/10.1016/j.jtrangeo.2015.08.006

El-Geneidy A, Levinson D, Diab E, et al., 2016. The cost of equity: assessing transit accessibility and social disparity using total travel cost. *Transportation Research Part A: Policy and Practice*, 91:302-316. https://doi.org/10.1016/j.tra.2016.07.003

Farber S, Fu LW, 2017. Dynamic public transit accessibility using travel time cubes: comparing the effects of infrastructure (dis)investments over time. *Computers, Environment and Urban Systems*, 62:30-40. https://doi.org/10.1016/j.compenvurbsys.2016.10.005

GaWC (Globalization and World Cities), 2016. The World According to GaWC 2016. Loughborough University, UK. https://www.lboro.ac.uk/microsites/geography/gawc/world2016.html

Ge ZY, Gao P, 2008. Studies on traffic effects of high-speed ring road in city center. *Kybernetes*, 37(9-10):1315-1321. https://doi.org/10.1108/03684920810907607

Geroliminis N, Sun J, 2011. Properties of a well-defined macroscopic fundamental diagram for urban traffic. *Transportation Research Part B: Methodological*, 45(3):605-617. https://doi.org/10.1016/j.trb.2010.11.004

Geurs KT, van Wee B, 2004. Accessibility evaluation of land-use and transport strategies: review and research directions. *Journal of Transport Geography*, 12(2):127-140. https://doi.org/10.1016/j.jtrangeo.2003.10.005

Gutiérrez J, González R, Gómez G, 1996. The European high-speed train network: predicted effects on accessibility patterns. *Journal of Transport Geography*, 4(4):227-238. https://doi.org/10.1016/S0966-6923(96)00033-6

Hansen WG, 1959. How accessibility shapes land use. *Journal of the American Institute of Planners*, 25(2):73-76. https://doi.org/10.1080/01944365908978307

Hielkema H, Hongisto P, 2013. Developing the Helsinki smart city: the role of competitions for open data applications. *Journal of the Knowledge Economy*, 4(2):190-204. https://doi.org/10.1007/s13132-012-0087-6

Imhoff ML, Lawrence WT, Stutzer DC, et al., 1997. A technique for using composite DMSP/OLS "City Lights" satellite data to map urban area. *Remote Sensing of Environment*, 61(3):361-370.

https://doi.org/10.1016/S0034-4257(97)00046-1

Irons JR, Dwyer JL, Barsi JA, 2012. The next landsat satellite: the landsat data continuity mission. *Remote Sensing of Environment*, 122:11-21. https://doi.org/10.1016/j.rse.2011.08.026

Jäppinen S, Toivonen T, Salonen M, 2013. Modelling the potential effect of shared bicycles on public transport travel times in Greater Helsinki: an open data approach. *Applied Geography*, 43:13-24. https://doi.org/10.1016/j.apgeog.2013.05.010

Koopmans C, Rietveld P, Huijg A, 2012. An accessibility approach to railways and municipal population growth, 1840-1930. *Journal of Transport Geography*, 25:98-104. https://doi.org/10.1016/j.jtrangeo.2012.01.031

Kotavaara O, Antikainen H, Marmion M, et al., 2012. Scale in the effect of accessibility on population change: GIS and a statistical approach to road, air and rail accessibility in Finland, 1990-2008. *Geographical Journal*, 178(4): 366-382. https://doi.org/10.1111/j.1475-4959.2012.00460.x

Kwan MP, Murray AT, O'Kelly ME, et al., 2003. Recent advances in accessibility research: representation, methodology and applications. *Journal of Geographical Systems*, 5(1):129-138. https://doi.org/10.1007/s101090300107

Langford M, Higgs G, Radcliffe J, et al., 2008. Urban population distribution models and service accessibility estimation. *Computers, Environment and Urban Systems*, 32(1): 66-80. https://doi.org/10.1016/j.compenvurbsys.2007.06.001

Levine J, Garb Y, 2002. Congestion pricing's conditional promise: promotion of accessibility or mobility? *Transport Policy*, 9(3):179-188. https://doi.org/10.1016/S0967-070X(02)00007-0

Lu YM, Tang JM, 2004. Fractal dimension of a transportation network and its relationship with urban growth: a study of the Dallas-Fort Worth area. *Environment and Planning B: Planning and Design*, 31(6):895-911. https://doi.org/10.1068/b3163

Lu ZM, Zhang H, Southworth F, et al., 2016. Fractal dimensions of metropolitan area road networks and the impacts on the urban built environment. *Ecological Indicators*, 70:285-296. https://doi.org/10.1016/j.ecolind.2016.06.016

Lyons G, Urry J, 2005. Travel time use in the information age. *Transportation Research Part A: Policy and Practice*, 39(2-3):257-276. https://doi.org/10.1016/j.tra.2004.09.004

Ma T, Zhou CH, Tao P, et al., 2012. Quantitative estimation of urbanization dynamics using time series of DMSP/OLS nighttime light data: a comparative case study from China's cities. *Remote Sensing of Environment*, 124:99-107. https://doi.org/10.1016/j.rse.2012.04.018

Magruder JR, 2010. Intergenerational networks, unemployment, and persistent inequality in South Africa. *American Economic Journal: Applied Economics*, 2(1):62-85. https://doi.org/10.1257/app.2.1.62

Mallinckrodt J, 2010. VCI, a regional volume/capacity index model of urban congestion. *Journal of Transportation Engineering*, 136(2):110-119. https://doi.org/10.1061/(asce)te.1943-5436.0000080

Martens K, di Ciommo F, 2017. Travel time savings, accessibility gains and equity effects in cost–benefit analysis. *Transport Reviews*, 37(2):152-169. https://doi.org/10.1080/01441647.2016.1276642

Mavoa S, Witten K, McCreanor T, et al., 2012. GIS based destination accessibility via public transit and walking in Auckland, New Zealand. *Journal of Transport Geography*, 20(1):15-22. https://doi.org/10.1016/j.jtrangeo.2011.10.001

Metz D, 2008. The myth of travel time saving. *Transport Reviews*, 28(3):321-336. https://doi.org/10.1080/01441640701642348

NBSC (National Bureau of Statistics of China), 2016. China City Statistical Yearbook. China Statistics Press, Beijing, China.

Niedzielski MA, Boschmann EE, 2014. Travel time and distance as relative accessibility in the journey to work. *Annals of the Association of American Geographers*, 104(6):1156-1182. https://doi.org/10.1080/00045608.2014.958398

Noora CL, Afari EA, Nuoh RD, et al., 2016. Pedestrians' adherence to road traffic regulations on the N1 Highway in Accra, Ghana. *The Pan African Medical Journal*, 25(S1): 11. https://doi.org/10.11604/pamj.supp.2016.25.1.6184

Odoki JB, Kerali HR, Santorini F, 2001. An integrated model for quantifying accessibility-benefits in developing countries. *Transportation Research Part A: Policy and Practice*, 35(7):601-623. https://doi.org/10.1016/S0965-8564(00)00010-0

Rahmani M, Koutsopoulos HN, Jenelius E, 2017. Travel time estimation from sparse floating car data with consistent path inference: a fixed point approach. *Transportation Research Part C: Emerging Technologies*, 85:628-643. https://doi.org/10.1016/j.trc.2017.10.012

Rojas C, Páez A, Barbosa O, et al., 2016. Accessibility to urban green spaces in Chilean cities using adaptive thresholds. *Journal of Transport Geography*, 57:227-240. https://doi.org/10.1016/j.jtrangeo.2016.10.012

Saghapour T, Moridpour S, Thompson RG, 2016. Public transport accessibility in metropolitan areas: a new approach incorporating population density. *Journal of Transport Geography*, 54:273-285. https://doi.org/10.1016/j.jtrangeo.2016.06.019

Salonen M, Toivonen T, 2013. Modelling travel time in urban networks: comparable measures for private car and public transport. *Journal of Transport Geography*, 31:143-153. https://doi.org/10.1016/j.jtrangeo.2013.06.011

Sanaullah I, Quddus M, Enoch M, 2016. Developing travel time estimation methods using sparse GPS data. *Journal of Intelligent Transportation Systems: Technology, Planning, and Operations*, 20(6):532-544. https://doi.org/10.1080/15472450.2016.1154764

Sathisan SK, Srinivasan N, 1998. Evaluation of accessibility of urban transportation networks. *Transportation Research Record: Journal of the Transportation Research Board*, 1617(1):78-83. https://doi.org/10.3141/1617-11

Šenk E, Ambros J, 2011. Estimation of accident frequency at newly-built roundabouts in the Czech Republic. *Transactions on Transport Sciences*, 4(4):199-206. https://doi.org/10.2478/v10158-011-0018-4

Shi CY, Chen BY, Li QQ, 2017. Estimation of travel time distributions in urban road networks using low-frequency floating car data. *ISPRS International Journal of Geo-Information*, 6(8):253. https://doi.org/10.3390/ijgi6080253

Shi KF, Chen Y, Yu BL, et al., 2016. Detecting spatiotemporal dynamics of global electric power consumption using DMSP-OLS nighttime stable light data. *Applied Energy*, 184:450-463. https://doi.org/10.1016/j.apenergy.2016.10.032

Shirgaokar M, 2014. Employment centers and travel behavior: exploring the work commute of Mumbai's rapidly motorizing middle class. *Journal of Transport Geography*, 41:249-258. https://doi.org/10.1016/j.jtrangeo.2014.10.003

Silva C, Pinho P, 2010. The structural accessibility layer (SAL): revealing how urban structure constrains travel choice. *Environment and Planning A: Economy and Space*, 42(11):2735-2752. https://doi.org/10.1068/a42477

Small C, Lu JWT, 2006. Estimation and vicarious validation of urban vegetation abundance by spectral mixture analysis. *Remote Sensing of Environment*, 100(4):441-456. https://doi.org/10.1016/j.rse.2005.10.023

Spence N, Linneker B, 1994. Evolution of the motorway network and changing levels of accessibility in Great Britain. *Journal of Transport Geography*, 2(4):247-264. https://doi.org/10.1016/0966-6923(94)90049-3

Su Q, 2011. The effect of population density, road network density, and congestion on household gasoline consumption in U.S. urban areas. *Energy Economics*, 33(3):445-452. https://doi.org/10.1016/j.eneco.2010.11.005

Taylor MC, Lynam DA, Baruya A, 2000. The Effects of Drivers' Speed on the Frequency of Road Accidents. TRL Report 421, Transport Research Laboratory, Crowthorne, UK.

Taylor PJ, 2001. Specification of the world city network. *Geographical Analysis*, 33(2):181-194. https://doi.org/10.1111/j.1538-4632.2001.tb00443.x

Wan N, Zou B, Sternberg T, 2012. A three-step floating catchment area method for analyzing spatial access to health services. *International Journal of Geographical Information Science*, 26(6):1073-1089. https://doi.org/10.1080/13658816.2011.624987

Wang FH, Xu YQ, 2011. Estimating O-D travel time matrix by Google Maps API: implementation, advantages, and implications. *Annals of GIS*, 17(4):199-209. https://doi.org/10.1080/19475683.2011.625977

Weber J, 2018. Route change on the American freeway system. *Journal of Transport Geography*, 67:12-23. https://doi.org/10.1016/j.jtrangeo.2018.01.003

Weiss DJ, Nelson A, Gibson HS, et al., 2018. A global map of travel time to cities to assess inequalities in accessibility in 2015. *Nature*, 553(7688):333-336. https://doi.org/10.1038/nature25181

Ye CD, Hu LQ, Li M, 2018. Urban green space accessibility changes in a high-density city: a case study of Macau from 2010 to 2015. *Journal of Transport Geography*, 66:106-115. https://doi.org/10.1016/j.jtrangeo.2017.11.009

Yildirimoglu M, Geroliminis N, 2013. Experienced travel time prediction for congested freeways. *Transportation Research Part B: Methodological*, 53:45-63. https://doi.org/10.1016/j.trb.2013.03.006

Zha Y, Gao J, Ni S, 2003. Use of normalized difference built-up index in automatically mapping urban areas from TM imagery. *International Journal of Remote Sensing*, 24(3):583-594. https://doi.org/10.1080/01431160304987

Zhang J, Li PJ, Wang JF, 2014. Urban built-up area extraction from Landsat TM/ETM+ images using spectral information and multivariate texture. *Remote Sensing*, 6(8):7339-7359. https://doi.org/10.3390/rs6087339

Zhang Q, Wang J, Peng X, et al., 2002. Urban built-up land change detection with road density and spectral information from multi-temporal Landsat TM data. *International Journal of Remote Sensing*, 23(15):3057-3078. https://doi.org/10.1080/01431160110104728

Zhou YY, Smith SJ, Elvidge CD, et al., 2014. A cluster-based method to map urban area from DMSP/OLS nightlights. *Remote Sensing of Environment*, 147:173-185. https://doi.org/10.1016/j.rse.2014.03.004